JOURNAL OF MATERIALS SCIENCE 25 (1990) 137–143

Characterization of sputtered Inconel 617

Part 1 *Coatings in plan section*

MARIO EMILIANI
Pratt and Whitney, P.O. Box 109600, MS 707-28, West Palm Beach, Florida 33410, USA
MARC RICHMAN
Division of Engineering, Brown University, Box D, Providence, Rhode Island 02912, USA
RICHARD BROWN
Department of Chemical Engineering, University of Rhode Island, Kingston, Rhode Island 02881, USA

Inconel 617 coatings 10 to 13 μm thick were r.f. magnetron sputtered on to commercially pure α-titanium substrates without external bias or heat and examined in the as-deposited condition by scanning electron microscopy (SEM), analytical transmission electron microscopy (TEM) and X-ray diffraction (XRD). The surface finish of coatings was smooth with few nodular growth defects, while bend tests showed the coatings failed in a ductile manner. TEM showed that Inconel 617 coatings consisted of an fcc solid solution with an average lattice parameter of 0.366 nm. The through-thickness microstructure contained equiaxed grains with an average diameter of 50 nm, while XRD showed the coatings had a (1 1 1) orientation with respect to the substrate. Coatings contained a large amount of interfacial area, and had an average Knoop microhardness of 503 kg mm^{-2}.

1. Introduction

Inconel 617 (UNS N00617) is a nickel-based superalloy used in high-temperature environments ($\sim$ 1000° C) due to its excellent mechanical stability and oxidation and corrosion resistance. Primary industrial applications are in the aerospace and chemical industries, and fossil and nuclear power generation [1]. This alloy is a face-centred cubic (fcc) solid solution of nickel (52 wt %), chromium (22 wt %), cobalt (12 wt %), and molybdenum (9 wt %), with small amounts (< 1.5 wt % each) of iron, silicon, titanium and aluminium. The nominal chemical composition is given in Table I.

Studies of the microstructure and phase stability of bulk Inconel 617 have been reported previously [2, 3], but are summarized here to provide a background for the discussion of sputtered Inconel 617 coatings. The as-received microstructure of solution-annealed Inconel 617 consists of large equiaxed γ grains, ASTM 5 (65 μm average diameter) or coarser, with grain boundary $M_{23}C_6$ (M = Cr, Mo) and intragranular MC carbides (M = Ti). Bulk Inconel 617 is not γ' strengthened in the solution-annealed condition, but will undergo slight strengthening after lengthy exposure to temperatures above 650° C, primarily due to extensive precipitation of intragranular $M_{23}C_6$ (M = Cr + Mo) [2]. A more recent study has shown that eta-carbide, M_6C (M = Mo, Ni, Si), is precipitated primarily upon pre-existing $M_{23}C_6$ after heat treatment at 800° C [3]. No topologically close packed (tcp) phases such as σ, χ, or μ have been identified [2, 3]. Photomicrographs representative of the microstructure of this alloy before and after heat treatment are shown in Figs 1a to d.

TABLE I Nominal chemical composition (wt %) of Inconel 617 [1]

Ni	Cr	Co	Mo	Fe	Al	Mn	Si	Ti	Cu	C	S
52.0	22.0	12.5	9.0	1.5	1.2	0.5	0.5	0.3	0.2	0.07	0.008

The present study is part of an investigation of the microstructure and phase stability of both as-received bulk and sputtered Inconel 617, in which the latter was characterized for potential use as an oxidation, corrosion, or erosion resistant coating [4]. The reader is referred to the literature for examples of the application of coatings in gas turbine engines [5]. The phase stability of sputtered Inconel 617 coatings will be published separately [6].

2. Experimental procedure

2.1. Substrate material and preparation

Inconel 617 coatings were deposited on to commercially pure α-titanium sheet (ASTM B265079 Grade 1). This substrate material contains equiaxed grains 10 to 20 μm in diameter and fine titanium hydride needles, as shown in Figs 2a and b, respectively. Its chemical composition is listed in Table II. Inconel 617 was

TABLE II Nominal chemical composition wt % of α-titanium [4]

Ti	Fe	O	C	N	H
99.50	0.20	0.18	0.08	0.03	0.015

0022–2461/90 $03.00 + .12

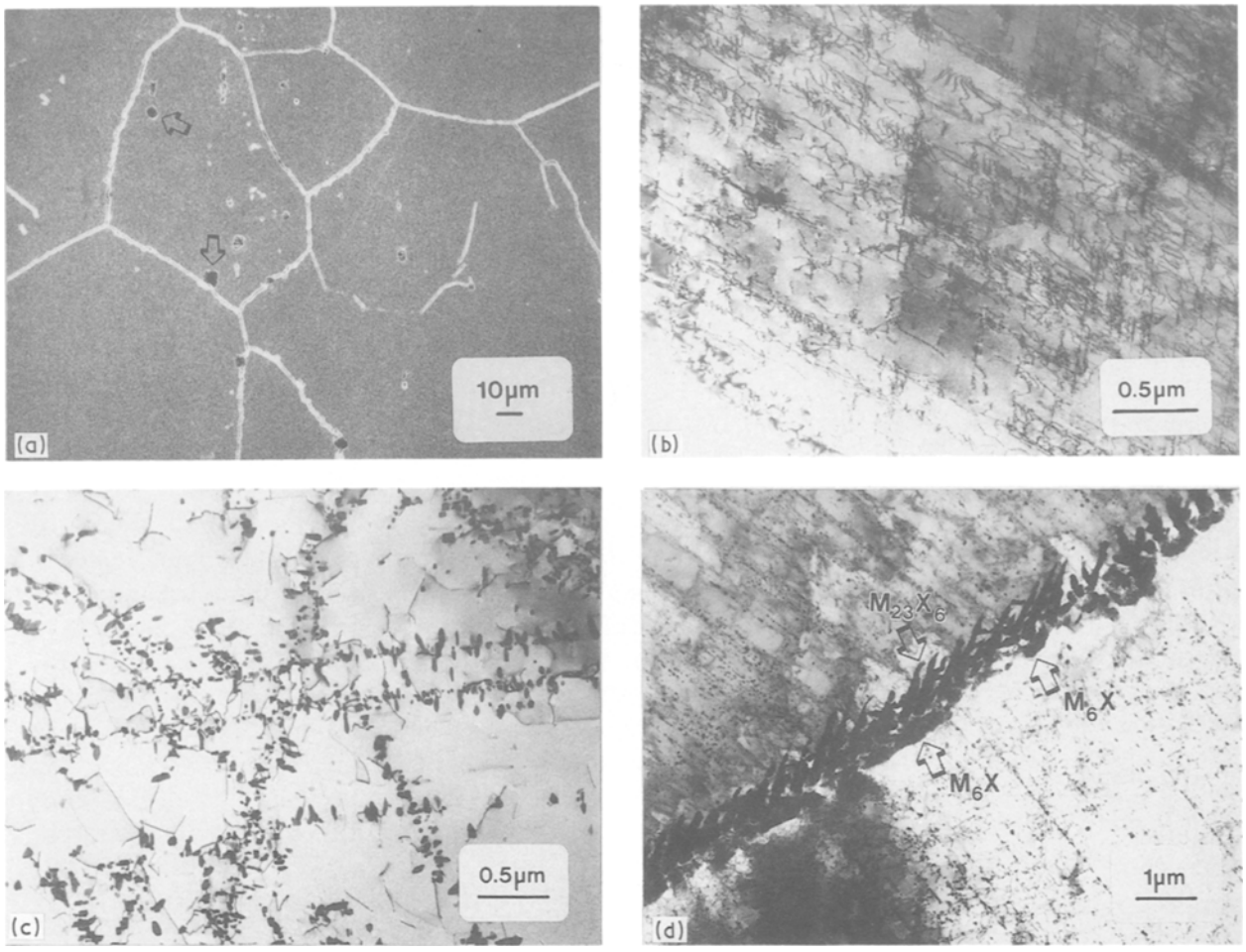

Figure 1 (a) Scanning electron micrograph of cold-rolled and solution-annealed Inconel 617 in the as-received condition showing grain boundary and intragranular carbide (arrows). Etched in glyceregia. (b) Dislocations in the γ phase of as-received Inconel 617. (c) Intragranular $M_{23}C_6$ nucleated upon slip lines and dislocations after heat treatment at 800° C for 200 h. (d) M_6C nucleated on grain boundary $M_{23}C_6$ (arrows). Note the extensive precipitation of intragranular $M_{23}C_6$.

deposited on to ground (30 μm SiC) titanium sheet 0.5 mm thick for evaluation of coating defects, adherence, and ductility by SEM. Coatings were also deposited on to metallographically polished titanium discs, 3 mm in diameter and about 100 μm thick, for TEM studies. All substrates were ultrasonically cleaned for 5 min each in trichloroethane, acetone, and ethanol, immediately inserted into the sputtering unit, and a vacuum of better than 3×10^{-6} torr was achieved.

2.2. Sputtering

Sputtering was performed in a Materials Research Corporation model 8667 + 2M 1.5 kW radio frequency (13.56 MHz) sputtering unit. The vacuum chamber was silicone oil diffusion pumped and equipped with a liquid nitrogen cold trap. Cold-rolled and solution-annealed Inconel 617 plate 0.64 cm thick was machined into a circular disc 14.6 cm diameter and bonded to a water-cooled OFHC copper magnetron backing plate using conducting silver-filled

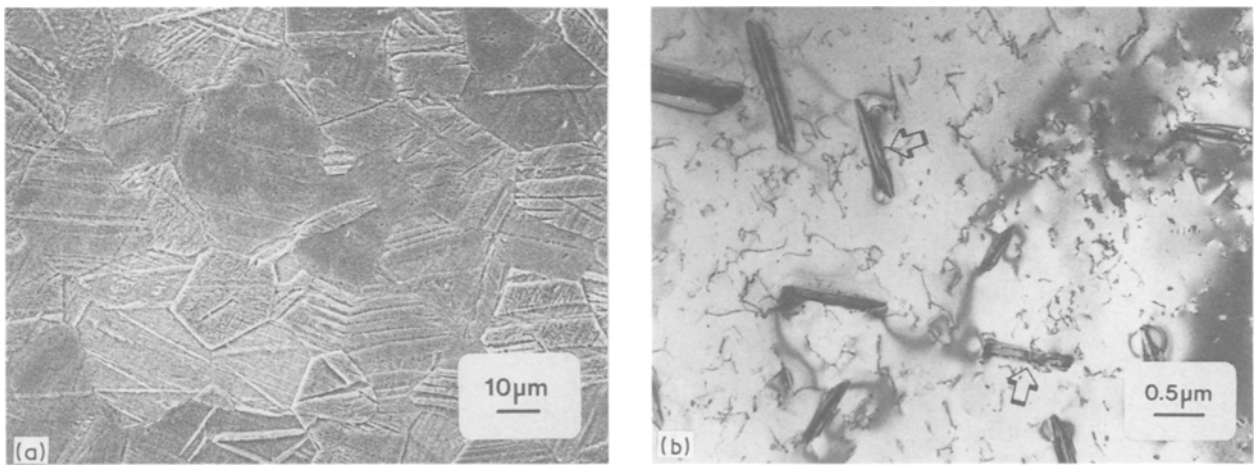

Figure 2 (a) Scanning electron micrograph of commercially pure α-titanium showing small equiaxed grains, twins, and titanium hydride precipitates (Etched in Kroll's solution). (b) Transmission electron micrograph of titanium hydride needles (arrows).

epoxy cement. Ultra-high purity (UHP) argon (99.999%) was used for sputter-cleaning, target presputtering, and deposition of Inconel 617 coatings. The substrates and vacuum chamber walls were sputter-cleaned for 10 min in argon using a forward r.f. of 1000 W and a working gas pressure of 15 mtorr at a volumetric flow rate of 19.20 $cm^3 sec^{-1}$. Substrates were shielded from the target which was then sputter-cleaned for 10 min at 1000 W forward r.f. and 2 mtorr argon at 19.20 $cm^3 sec^{-1}$. The optimum sputtering conditions were found to be a forward r.f. of 1000 W and an argon gas pressure of 2 mtorr at 19.20 $cm^3 sec^{-1}$, resulting in an average deposition rate of 180 nm min^{-1} (0.18 $\mu m\ min^{-1}$) as determined by step profilometry. These conditions produced an average power density of 6 W cm^{-2}, 440 V across the electrodes, 2.27 A discharge current, and 13.5 mA cm^{-2} discharge current density. Coatings 10 to 13 μm thick (depending upon location below the target) were deposited in 75 min.

The substrates were not externally biased during deposition, and are therefore assumed to have been at ground potential during sputtering. Samples were placed upon a water-cooled platform and were not externally heated. A thermocouple in contact with the water-cooled platform and placed adjacent to the substrates during sputtering recorded a maximum temperature of 320° C, resulting in a homologous temperature of $T/T_m = 0.36$. Substrates were cooled under vacuum for a minimum of 2 h after sputtering. Numerous depositions and subsequent microstructural analyses showed that the above parameters resulted in reproducible and high-quality adherent coatings up to 34 μm thick.

2.3. Electron microscopy

Scanning electron microscopy was performed in an AMR 1000A SEM at 20 keV. Analytical electron microscopy was performed using a Philips 420T scanning transmission electron microscope (STEM) at 120 keV, and equipped with a LaB_6 electron gun, EDAX System 9100/60 energy dispersive X-ray spectrometer (beryllium window), and a Gatan Model 607 electron energy loss spectrometer (EELS). The microscope was operated in TEM mode and aligned prior to each use to ensure reproducible conditions for magnification, diffraction camera length, and energy dispersive microanalysis.

The lattice parameter of sputtered coatings was determined by averaging the *d*-spacings of rings and spots from selected-area and convergent-beam electron diffraction patterns, respectively. Phase compositions were determined by quantitative energy dispersive spectroscopy (EDS) of $K\alpha$ lines using EDAX LIST halographic background stripping program and EDAX THIN software package employing the ratio method of analysis [7]. A minimum of 5000 counts full-scale at a count rate of < 2500 counts/sec was used for all energy dispersive spectra analysed quantitively. The elements of interest were "windowed" with an integrated intensity equal to 1.2 FWHM, and machine-generated *k*-values were used.

The microstructure of Inconel 617 coatings was examined through-thickness by dimpling the uncoated side of 3 mm titanium discs with a series of alumina slurries using a VCR Group Model D500 dimpler. Dimpling was stopped at the onset of perforation, at which time a hole about 0.5 mm diameter was produced in the coating. Samples were then argon ion milled without external cooling in a Gatan Model 600 twin gun ion mill to produce electron-transparent regions. The ion-milling conditions employed were a 10° gun angle, 5 kV gun voltage, 0.75 mA gun current, and 30 to 40 μA specimen current for 30 to 60 min. This method reveals a microstructure representative of that about 1 μm below the surface of the coating.

EELS was used to determine the presence of argon, carbon, nitrogen and oxygen in sputtered coatings. However, samples were prepared by methods different from that given above (i.e. jet polishing) in order to eliminate artefacts such as argon from ion milling. Coatings 10 to 13 μm thick were peeled from 23 μm thick molybdenum foil substrates, mechanically punched into 3 mm discs, and jet polished using a Struers Tenupol-2 twin jet electropolishing unit. A solution of 25% nitric acid (HNO_3) in methanol was used as the electrolyte and maintained at −30° C using Klein-Kryomat refrigeration system. Typical electropolishing conditions were 6 V and a current of 80 mA for 20 to 30 sec. These coatings were found to contain the same microstructure as that deposited on to titanium substrates.

3. Results and discussion

3.1. SEM of as-sputtered Inconel 617 coatings

Coatings on ground substrates were smoother than the surface finish of the initial substrate as determined by step profilometry. This is in contrast to most studies where the coating was found to faithfully replicate or even amplify surface irregularities in the absence of external bias and at low T/T_m [8, 9]. Nodular growth defects were occasionally observed on both ground and polished substrates, Figs 3a and b, but were generally rare in both cases. This is in contrast to studies showing that the formation of nodular growth defects is strongly dependent on surface finish [9]. Most growth nodules found in this study are attributed to embedded SiC and Al_2O_3 grinding and polishing abrasives, respectively, and other foreign debris on the substrate. The low number of defects and smooth surface finish are evidence of high adatom mobility, indicating the microstructure may be more indicative of a Zone 2 structure due to higher-than-measured substrate surface temperature and increased substrate bombardment [8, 9]. The density of coatings applied to polished titanium substrates was found to be the same as that of bulk Inconel 617 (8.36 g cm^{-3}).

The fracture morphology of coatings applied to 0.5 mm thick ground titanium substrates as determined by 180° bend tests showed that fracture did not initiate until samples were bent to an angle greater than 45°, and that coatings failed in a tortuous manner (Fig. 4a). Small dimples 0.2 to 0.5 μm diameter were indicative of ductile failure (Fig. 4b). Coatings

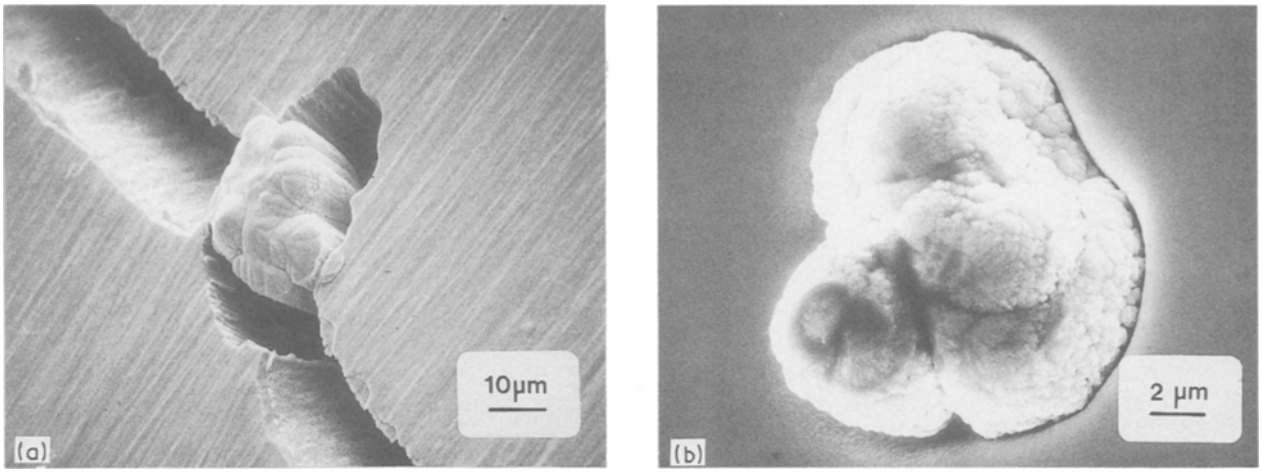

Figure 3 (a) Scanning electron micrograph of a nodular growth defect in sputtered Inconel 617 deposited on to ground α-titanium. Note that the coating has fractured around the growth defect in this bend test sample. (b) Scanning electron micrograph of a nodular growth defect in sputtered Inconel 617 deposited on to polished α-titanium. Note the smooth surface finish around the nodule.

were therefore strongly adherent to titanium substrates. However, fracture morphology is substrate-dependent. Much of the previous work determining the coating morphology has been on coatings applied to brittle substrates, which tend to show features more characteristic of microstructures as depicted in the Thornton Structural Zone Model [10]. Inconel 617 coatings deposited on glass and sapphire substrates showed a similar dependence; i.e. the coatings exhibited a columnar fracture morphology corresponding to both low T/T_m and working gas pressure.

The average Knoop microhardness of coatings deposited on to polished α-titanium substrates was 503 kg mm^{-2} (100 g load). This corresponds to a Rockwell C hardness of approximately R_C 40 [11], as opposed to an average Rockwell B hardness of the as-received Inconel 617 sputtering target of R_B 88, and is indicative of a fine grain size in the coating. X-ray diffraction of the coating showed only one peak at $2\theta = 43.9°$ (Fig. 5), which corresponds to a d-spacing of 0.205 nm and indicates only (1 1 1) planes lying parallel to the substrate. This is consistent with other studies of copper and nickel coatings, in which the most dense crystal planes lie parallel to the substrate surface [12–14].

3.2. TEM of as-sputtered Inconel 617 coatings

TEM of the near-surface microstructure showed that the coatings were a solid solution with equiaxed γ grains ranging in size from 20 to 50 nm diameter (Fig. 6a). Grain boundaries are not clearly distinguishable due to high strain contrast and overlapping grains. A few grains as large as 150 nm in diameter were also found. In addition, the coating contained clusters of fine twins and stacking faults perpendicular to the substrate, Fig. 6b. Through-focus imaging did not reveal the presence of voids in the coating. This microstructure is similar to both sputtered nickel and copper [12, 13].

Quantitative stereological analysis of the microstructure using both area and intercept methods showed that there was an average of about 320 grains/μm^2 (3.2×10^8 grains/mm^2) with diameters of 40 to 60 nm. The grain-boundary density was calculated using the relationship:

$$S_v = 2P_L M \quad (1)$$

where S_v is the average grain boundary area per unit volume (cm^2 cm^{-3}), P_L is the average number of grain boundaries intercepted by a randomly placed straight line of known length, and M is the magnification of

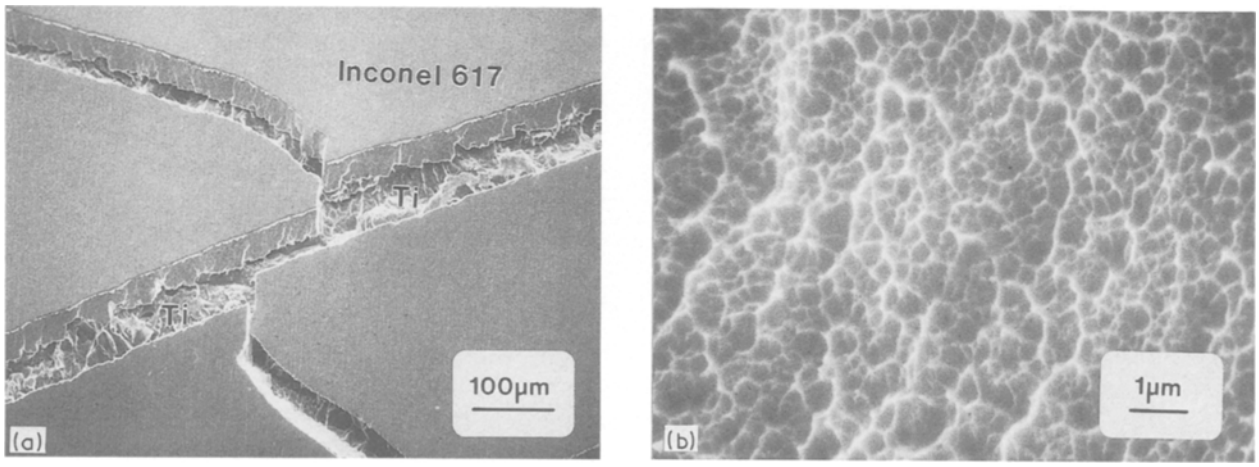

Figure 4 (a) Scanning electron micrograph showing the fracture morphology of as-sputtered Inconel 617 on ground α-titanium. (b) Scanning electron micrograph of ductile dimples in a bend test sample.

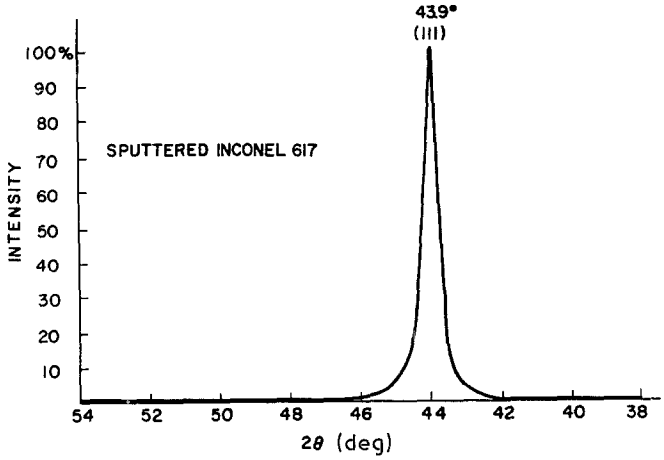

Figure 5 X-ray diffraction pattern of Inconel 617 sputtered on to ground α-titanium showing only [1 1 1] planes parallel to the substrate.

the micrograph [15]. The total average interfacial area was found to be $3.6 \times 10^6 cm^2 cm^{-3}$. If the width of the interfacial region is about 2 nm and the average grain size is 50 nm, then the volume fraction of grain-boundary material is about 15%. This is in contrast to conventional single-phase polycrystalline metals in which the volume fraction of interfacial material is only about 0.05% [16]. The significance of this with regards to the phase stability of this coating will be discussed in a separate publication [6].

A preliminary study indicated that the crystal structure of sputtered Inconel 617 was body-centred cubic [17]. The present, more detailed TEM investigation, however, shows that the structure is instead face-centred cubic with an average lattice parameter of 0.366 nm. Typical selected-area (SADP) and convergent-beam electron diffraction (CBED) patterns of the coating are shown in Figs 6c and d. The average lattice parameter of bulk solution annealed Inconel 617 is 0.362 nm; a difference of about 1% [3]. The continuous

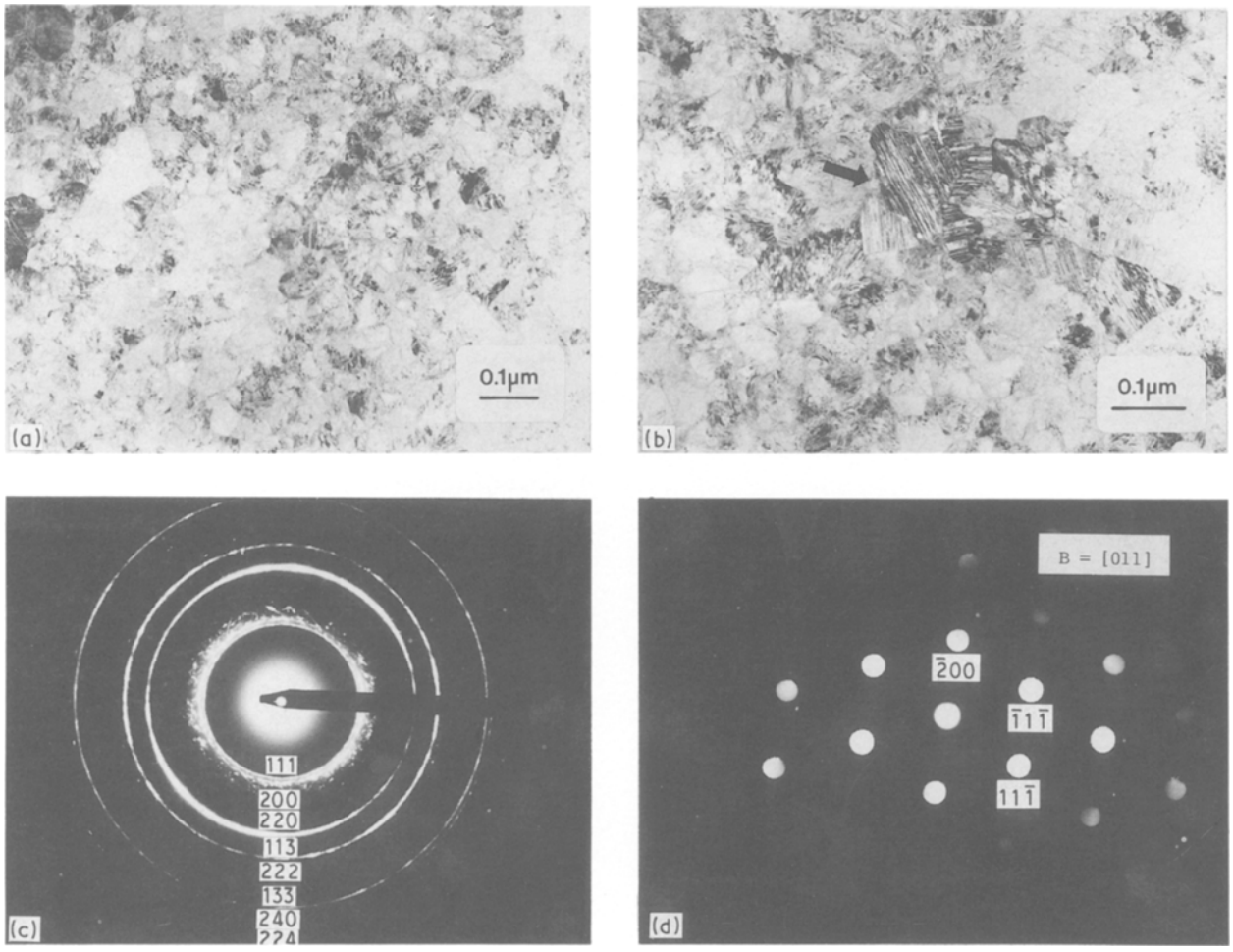

Figure 6 (a) Through-thickness transmission electron micrograph of as-sputtered Inconel 617 deposited on to polished α-titanium. Grains and grain boundaries are difficult to resolve due to the large amount of strain contrast. (b) Through thickness transmission electron micrograph showing clusters of twins and stacking faults perpendicular to the substrate (arrowed). (c) 2 μm SADP of as-sputtered Inconel 617. Note the diffuse fcc [1 1 1] and [2 0 0] rings, and [2 2 0] preferred orientation. (d) CBED of as-sputtered Inconel 617 showing the fcc [0 1 1] zone axis. (e) [1 1 1] + [2 0 0] dark-field transmission electron micrograph of as-sputtered Inconel 617. (f) [2 2 0] dark-field TEM of as-sputtered Inconel 617. A [2 2 0] preferred orientation is apparent compared to (e).

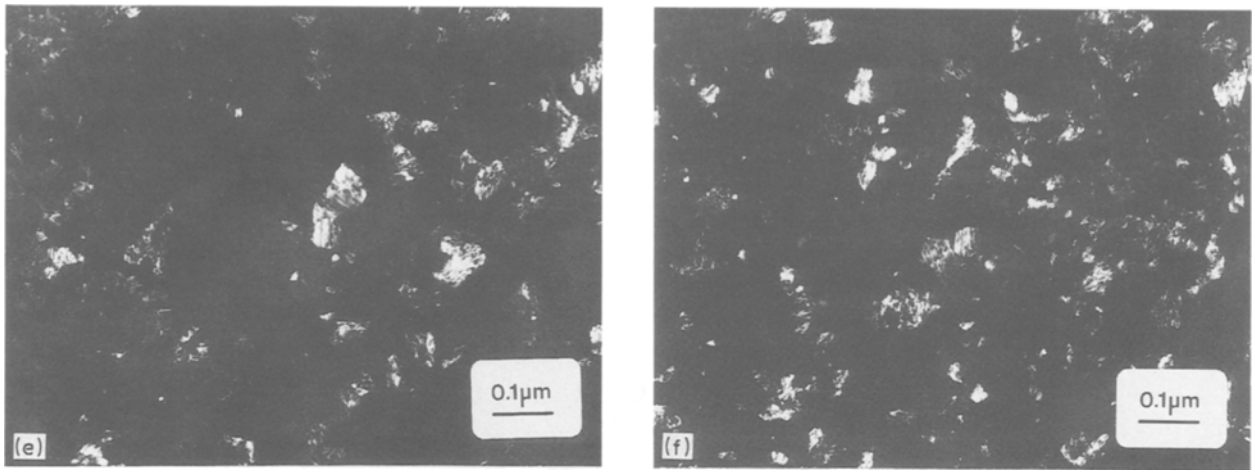

Figure 6 Continued

rings in Fig. 6c are indicative of a large number of grains contributing to the 2 μm selected-area diffraction pattern. A (2 2 0) preferred orientation is apparent in the SADP (Fig. 6c). Further, the (1 1 1) and (2 0 0) reflections are thickened and poorly defined due to the lack of (2 0 0) crystal orientations and the large amount of strain on (1 1 1) extrinsic stacking faults and twin planes, apparently resulting in inconsistent *d*-spacings. Higher order reflections (i.e. (4 0 0), (3 3 3), etc.) appear to be missing, but instead are simply faint. Dark-field imaging of (1 1 1) + (2 0 0) reflections (combined) and (2 2 0) reflections (alone) provided further evidence of (2 2 0) texture (Figs 6e, f).

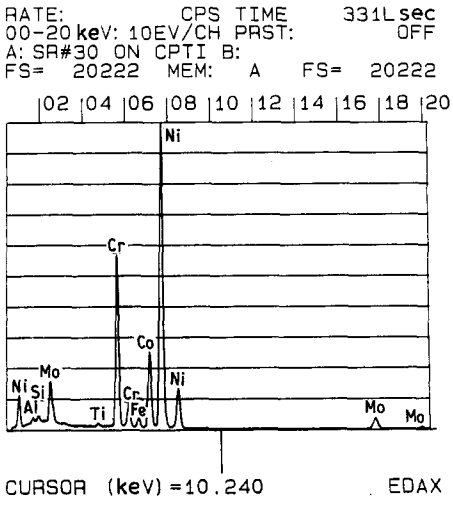

Figure 7 EDAX spectrum of as-sputtered Inconel 617.

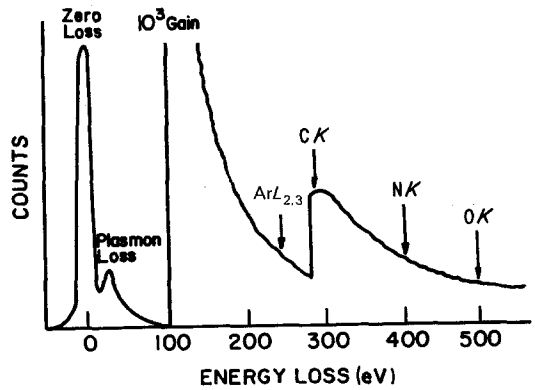

Figure 8 EELS spectrum showing the zero and plasmon electron loss features, and the location of $ArL_{2,3}$, C*K*, N*K*, and O*K* edges. The carbon signal is commensurate with that expected from sputtering carbides in the target.

Quantitative EDS showed the four primary alloying elements in the γ-phase to be 54.8 wt % Ni, 24.5 wt % Cr, 12.9 wt % Co, and 7.8 wt % Mo. A small amount ($\sim$ 1 wt % each) of iron, aluminium, silicon and titanium was also detected (Fig. 7). This composition differs slightly from that given by the supplier of the sputtering target used in this study (Table I), and is probably the result of overlapping *K*β lines, non-quantitative analysis of minor alloying elements, normal variations in alloy composition, and perhaps uncorrected ZAF.

Inconel 617 coatings were analysed for the presence of entrapped argon, carbon, oxygen, and nitrogen by EELS using jet-polished samples. The resultant energy loss spectrum is shown in Fig. 8. The magnitude of the C*K* edge is consistent with that expected in as-sputtered Inconel 617 coatings due to sputtering of refractory metal carbides (i.e. $M_{23}C_6$ and MC) in the target. No electron energy loss features indicative of the presence of argon, oxygen or nitrogen were detected.

4. Conclusion

Inconel 617 coatings 10 to 13 μm thick were r.f. magnetron sputtered in argon on to commercially pure α-titanium substrates without external bias or heat. Coatings were adherent, smooth, and mostly free of nodular growth defects. Bend tests produced dimples on coating fracture surfaces and are indicative of ductile failure. Coatings were an f c c solid solution with an average lattice parameter of 0.366 nm, compared to 0.362 nm for bulk solution-annealed Inconel 617. The through-thickness microstructure consisted of equiaxed γ grains an average of 50 nm diameter, resulting in a grain-boundary density of approximately 3.6 $\times$ 10^6 cm^2 cm^{-3}.

Acknowledgements

The authors thank the Division of Engineering and the Central Microscopy Facility at Brown University, the University of Rhode Island Department of Chemical Engineering, Monet Inc., and Pratt and Whitney for their support. Special thanks to Joe Fogarty.

References

1. "Inconel Alloy 617" (Huntington Alloys Inc., Huntington, West Virginia, 1979).
2. W. L. MANKINS, J. C. HOSIER and T. H. BASSFORD, *Metall. Trans.* **5** (1974) 2579.
3. M. EMILIANI, PhD thesis, Brown University, 1988.
4. MARIO L. EMILIANI, *ibid.* (1988).
5. Special issue: "Protective Coating Systems for High Temperature Gas Turbine Components", *Mater. Sci. Tech.* **3** (1986) 193.
6. M. EMILIANI, M. RICHMAN and R. BROWN, 'The Microstructure and Phase Stability of Sputtered Inconel 617' in preparation.
7. "EDAX PV9100/60 Quantitative Thin Section User's Manual", Version 2.3 (EDAX International Inc., Prairie View, Illinois, 1983).
8. J. A. THORNTON, *J. Vac. Sci. Technol.* **A4** (1986) 3059.
9. T. SPALVINS and W. A. BRAINARD, *ibid.* **11** (1974) 1186.
10. J. A. THORNTON, *ibid.* **11** (1974) 666.
11. G. F. VANDER VOORT, "Metallography" (McGraw-Hill, New York, 1984) Ch. 5.
12. S. D. DAHLGREN, *J. Vac. Sci. Technol.* **11** (1974) 832.
13. S. D. DAHLGREN, W. L. NICHOLSON, M. D. MERZ, W. BOLLMANN, J. F. DEVLIN and R. WANG, *Thin Solid Films* **40** (1977) 345.
14. R. W. VOOK and F. WITT, *J. Vac. Sci. Technol.* **2** (1965) 49.
15. R. T. DEHOFF and F. N. RHINES, "Quantitative Metallography" (McGraw-Hill, New York, 1968) Ch. 4.
16. P. M. FABIS, *J. Vac. Sci. Technol.* **A5** (1987) 75.
17. M. EMILIANI, M. RICHMAN, R. BROWN and O. GREGORY, *Surf. Coat. Tech.* **33** (1987) 267.

Received 27 September 1988
and accepted 27 February 1989